https://doi.org/10.37434/tpwj2021.06.04

STRUCTURE OF LASER WELDED JOINTS OF MULTICOMPONENT HIGH-ENTROPY ALLOY OF Nb–Cr–Ti–Al–Zr SYSTEM

V.D. Shelyagin[1], **A.V. Bernatskyi**[1], **O.V. Siora**[1], **V.I. Bondareva**[1] and **M.P. Brodnikovskyi**[2]
[1]E.O. Paton Electric Welding Institute of the NAS of Ukraine
11 Kazymyr Malevych Str., 03150, Kyiv, Ukraine. E-mail: office@paton.kiev.ua
[2]I.M. Frantsevich Institute for Problems of Materials Science of the NAS of Ukraine
3 Krzhyzhanovskyi Str., 0312, Kyiv, Ukraine

In the work the authors studied the problems of laser welding of joints of high-entropy alloy of Nb–Cr–Ti–Al–Zr system. The results of differential thermal analysis of the initial material are presented. Results of X-ray phase analysis of the alloy were analyzed. A conclusion was made about existence of bcc solid solution based on niobium and solid solution based on $ZrCr_2$ intermetallics in the alloy, as well as existence of two niobium-based solid solutions with different chemical composition in the alloy. Analysis of the influence of alloy crystallization rate on its microstructure was performed. It is shown that the ratio of the quantity of dendrites and eutectic can change, depending on the cooling rate. Obtained results of investigations on formation of a dendrite structure were furtheron used at optimization of laser welding modes. In this work the authors studied the influence of such parameters as radiation power and laser welding speed on weld microstructure formation. Mechanical properties of butt joints at uniaxial static tension were studied. It was found that material softening which leads to destruction is influenced by the feature of distribution of residual thermal stresses that is determined by the mode of heat input and removal during welding. It is shown that formation of the majority of the defects is related to a feature of nonequilibrium crystallization of multicomponent high-entropy high-temperature alloys. In order to prevent their formation, it is rational to take measures for optimizing the technology parameters, aimed at increasing the melt cooling rate, in order to produce a more equilibrium structure. 15 Ref., 5 Figures.

Keywords: multicomponent high-entropy alloy, laser welding, butt joints, structure, mechanical properties, defects

Many researchers maintain that the possibilities of the traditional approaches to development of new alloys and technologies have largely been exhausted and no longer lead to any essential increase of the properties [1–3]. So, development of metallic materials consists in selection of alloying elements to obtain the necessary characteristics of the alloy, based on one component. However, the variability in selection of alloying elements already is practically limited. At the same time, technologies of product manufacturing in many respects do not take into account the peculiarities of phase formation during processing, multilevel nature of the structure, scale and distribution of structural elements that often does not allow reaching the high values of mechanical and technological properties of the alloys and their optimal balance.

At present so-called high-entropy alloys attract the attention of material scientists all over the world [4–6]. This interest is due to several factors. First, the concept of high-entropy alloys opens up great possibilities for creation of new alloys with the structures and properties, differing from those for the «traditional» alloys. Secondly, some of the already studied alloys have demonstrated extremely attractive mechanical properties: combination of high ductility and strength at room temperature, record values of impact toughness and fracture toughness at room and cryogenic temperatures, high specific strength at higher temperatures, etc. [7–9]. Such an approach to searching for new compositions reveals one more direction of research, owing to a huge number of possible variants of the alloy compositions.

Multicomponent high-temperature alloys with niobium also belong to novel promising materials. At present they are becoming ever wider applied in manufacture of individual parts of experimental and test products and mock-ups for aerospace and power engineering [10–12]. Absence of reliable technologies of joining multicomponent high-temperature alloys with niobium limits the introduction of these alloys in the industrial sector of the economy. Welding of multicomponent high-temperature alloys with niobium is complicated in connection with formation of intermetallics during weld metal cooling, as well as possible

V.D. Shelyagin — https://orcid.org/0000-0001-8153-6533, A.V. Bernatskyi — https://orcid.org/0000-0002-8050-5580,
O.V. Siora — https://orcid.org/0000-0003-1927-790X, V.I. Bondareva — https://orcid.org/0000-0002-4745-0995

formation of hydrates, nitrides and oxides that embrittle the metal of the weld and HAZ [13–15]. Data on producing permanent welded joints of high-entropy high-temperature alloys with niobium now are limited. There is an obvious lack of fundamental research which systematically correlate, on the one hand, the composition, structure, deformation and strengthening mechanisms, induced phase transformations, and on the other hand, mechanical and technological properties, depending on the welding modes. Thus, performance of such studies certainly is an urgent task for metals science and development of the technologies of manufacturing advanced technology products.

The objective of this work is establishing the regularities of formation of the structure of butt welded joints of multicomponent high-entropy alloy based on Nb–Cr–Ti–Al–Zr system, depending on laser welding modes.

Methods and equipment. Influence of cooling rate on the features of crystallization of a multicomponent high-entropy 36Nb–16Cr–16Ti–16Zr–16Al alloy was studied using laser melting. Radiation power, its movement speed and thickness of alloy plates allowed variation of the rate of heat input and removal at material melting. With this purpose bead-on-plate deposition was performed on 0.6–2.0 mm plates from multicomponent high-entropy 36Nb–16Cr–16Ti–16Zr–16Al alloy. Nd:YAG solid state «DY044» laser and «YLR-400-AC» fiber laser were used. The laser radiation power was varied in the range of 200–1000 W. Laser welding of butt welded joints on plates of $L \times B \times H$ 30×10×1.8 mm size was performed in the selected modes. Welding speed was varied from 50 to 1000 mm/min. The microstructure was studied on transverse sections and fractures by light microscopy («MIM-9» optical microscope with a digital attachment for image recording was used) and scanning electron microscopy («Superprob 733» electron microscope was used). Comparative X-ray structural analysis of the alloys was performed in «DRON-3M» diffractometer. Pictures were taken in CuK_α-radiation. Radiogram analysis by Rietveld was performed using PowderCell 2.4 software. The features of alloy melting were studied using the method of differential thermal analysis. Mechanical testing for static uniaxial tension were conducted in the vacuum of 10^{-3} Pa at the temperature of 1000 °C in a unit of 1246 type produced by the Research and Design Institute of Testing Machines, Instruments and Mass Measuring Devices.

Results and discussion. Result of studying the thermal effects at heating and cooling of the alloy, using differential thermal analysis (DTA) are given in Figure 1. At constant rate of furnace heating (20 °C/min) in the temperature range of 1400 °C, an abrupt lowering of the alloy temperature compared to furnace temperature, and at cooling — its abrupt rise in a narrow temperature range, are observed. A narrow temperature range and high value of thermal effect, its characteristic relative shifting by temperature at heating and cooling are typical for eutectic melting.

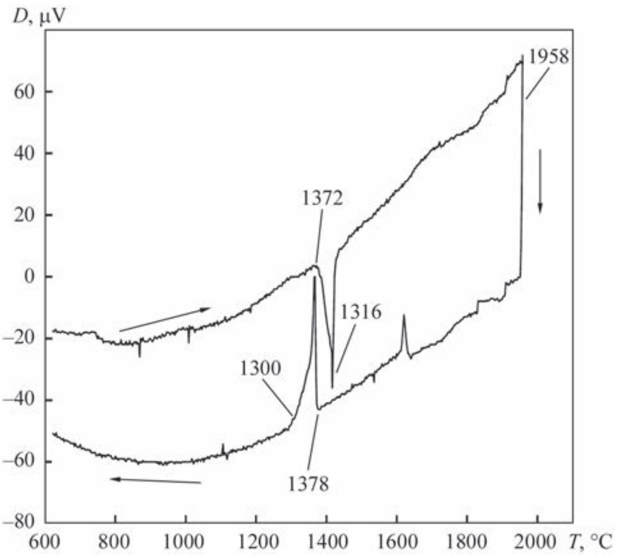

Figure 1. DTA curves at heating and cooling for 36Nb–16Cr–16Ti–16Zr–16Al alloy. The arrow shows the direction of temperature change

X-ray phase analysis (Figure 2) is indicative of the existence of bcc niobium-based solid solution and solid solution based on $ZrCr_2$ intermetallic in the alloy. Formation of solid solutions is indicated by shifting of the lines, corresponding to crystalline lattices of pure niobium and $ZrCr_2$. Bifurcation of the lines of bcc solid solution, which is readily fixed at increase of the scale, is indicative of existence of two niobium-based solid solutions with different chemical composition in the alloy.

Important factors for optimization of the procedure of welding of 36Nb–16Cr–16Ti–16Zr–16Al alloy are not only the above-described regularities of

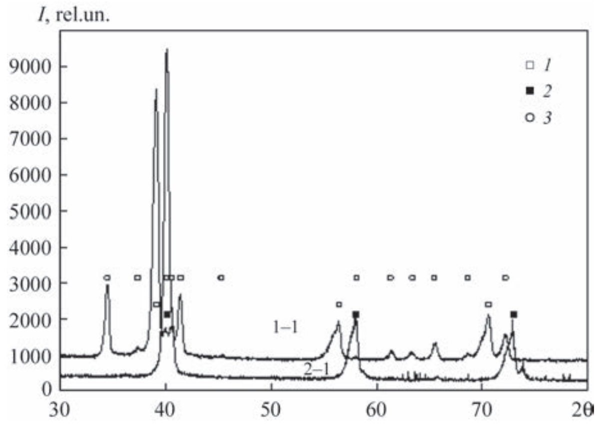

Figure 2. Roentgenographs of the following alloys: 1–1 — 36Nb–16Cr–16Ti–16Zr–16Al alloy; 2–1 — Nb: *1* — bcc phase in 1–1 alloy; *2* — bcc phase, niobium; *3* — $ZrCr_2$-based solid solution

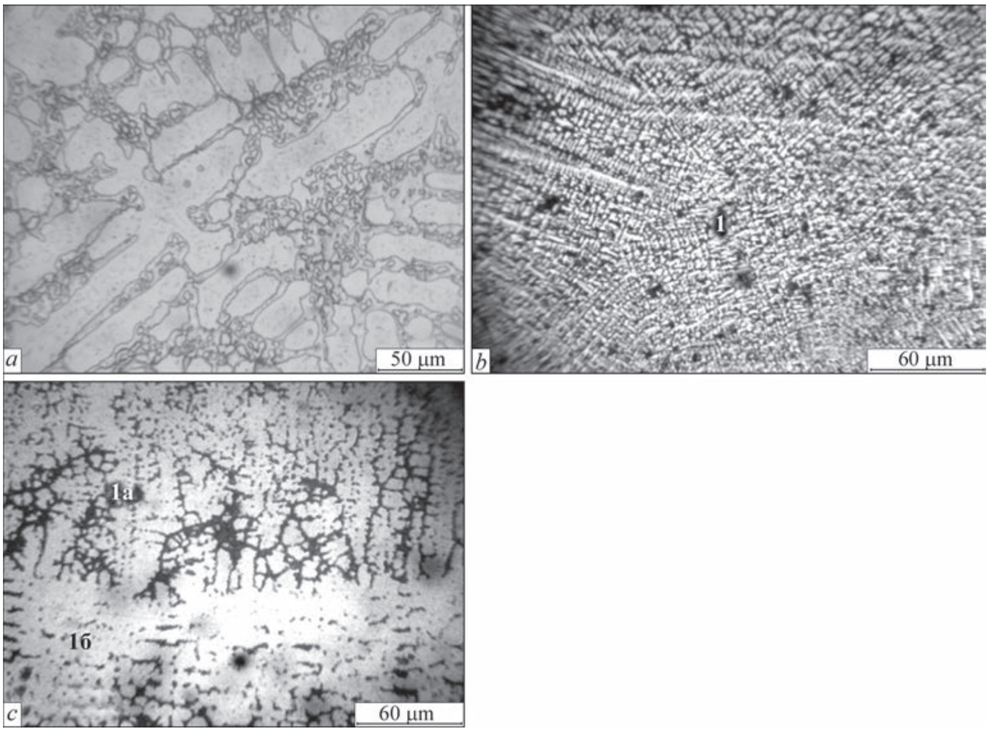

Figure 3. Microstructure of 36Nb–16Cr–16Ti–16Zr–16Al alloy, depending on crystallization rate (V_1): *a* — initial structure (after argon-arc melting) — V_1; *b* — V_2; *c* — V_3; $V_3 > V_2 > V_1$

phase composition formation at its crystallization, but also the established fact of nonmonotonic dependence of the size of the forming dendritic structure on the melt crystallization rate (Figure 3).

The alloy cooling was the slowest at melting in an argon-arc furnace. Even though the ingot lies on a copper tray which is water-cooled, the crystallization rate is reduced by a special mode of ingot heating by the arc to reduce the casting porosity and increase the chemical composition homogeneity. The alloy structure forms as a result of crystallization of dendrites which are niobium-based solid solution with increased content of the refractory components that changes the liquid phase composition. In Figure 3, *a* the primary dendrites are large grains of a light-coloured phase. Alloy intersection by microsection plane shows that the dendrites have the form of rods of 120–150 µm length, and 20–30 µm diameter. Both the dimensions of the rods are clearly revealed in the intersection of the alloy by microsection plane (Figure 3, *a*). Located between the dendrites is a mixture of fine grains of the two phases. This is the eutectic. The light-coloured fine grains between the dendrites are the niobium-based bcc solid solution that crystallized as an eutectic component at a lower temperature, than the primary dendrites. Change of the crystallization temperature of the two bcc phases, based on niobium, is associated with their different chemical composition that is fixed as bifurcation of the lines in the roentgenogram (Figure 2).

Increase of the cooling rate at crystallization leads to reduction of the size of primary dendrites. Diameter of the dendrite rods is equal to ~2 µm (Figure 3, *b*). Interdendritic gaps look like a dark phase as a result of light scattering on a mixture of very fine eutectic crystals, due to roughness of the surface created by them. At further increase of the crystallization rate the size of the dendrites starts increasing. The effect of partial hardening of the melt of initial composition is observed (Figure 3, *c*). However, the dendrites with an increased content of the refractory components are partially created (as indicated by the shape of some crystals of the light-coloured phase and formation of a eutectic as a result of local change in the chemical residual composition) after precipitation of primary dendrites of the melt (Figure 3, *c*). The cooling rate is high and the fine-crystalline eutectic looks as the dark-coloured phase.

The results of studying the formation of welded joint microstructure when optimizing the laser welding modes are shown in Figure 4.

At a low power of laser radiation (200–400 W), melting takes place only on part of the butt joint depth (Figure 4, *a*). Joining of the butt occurs to the penetration depth. Melt crystallization rate is high and nonuniform by the molten pool depth. At laser welding in the mode corresponding to the structure in Figure 4, *a* (laser radiation power of 400 W, welding speed of 0.833 mm/s (50 mm/min)), a fine-crystalline structure forms on the pool surface (Figure 4, *a*, zone 1), which corresponds to crystallization at speed V_2 in

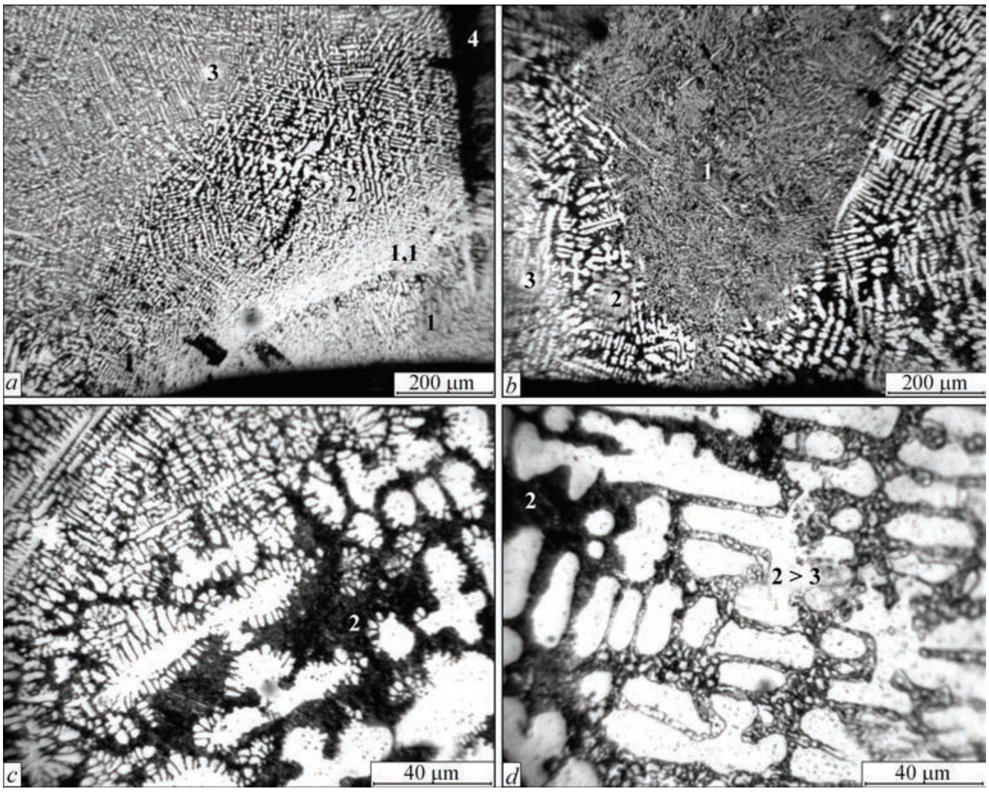

Figure 4. Alloy microstructure in laser welding zone: *a* — laser radiation power of 400 W; its movement speed of 0.833 mm/s (50 mm/min) at 1.8 mm thickness of welded plates; *b–d* — laser radiation power of 1000 W; its movement speed of 16.67 mm/s (1000 mm/min) at 1.8 mm thickness of welded plates

Figure 3, *b*. On the molten pool bottom the heat removal and, accordingly, the cooling rate, increase and a structure forms in the transition zone near the fusion line (Figure 4, *a*, zone 1–1), which corresponds to the structure produced in Figure 3, *c* at cooling rate V_3.

An increase of dendrite grain dimensions is observed in the HAZ (Figure 4, *a*, zone 2). Zone 3 corresponds to the material initial structure (Figure 4, *a*).

Change of the welding mode aimed at increase of the parameter values (laser radiation power of 1000 W, welding speed of 16.67 mm/s (1000 mm/min)), allows achieving complete penetration of a butt of plates of 1.8 mm thickness to the entire depth (Figure 4, *b*) and performing welding over the entire butt. In this case, the structure of zone 1 of complete melting is homogeneous. There is no unmolten metal on the pool bottom, which accelerates heat removal and changes the forming structure. An increase of the distance between the dendrites was revealed across the entire thickness of the welded butt joint in zone 2 — HAZ (Figure 4, *b*), which is observed as the appearance of a layer with increased content of the dark-coloured phase at transition from zone *1* (complete melting) to zone 3 (initial material) (Figure 4, *b*).

A confirmation of partial melting, just of the eutectic in the HAZ, is the growth during melt crystallization of dendrite branches of the second and third order at cooling on unmolten coarse dendrites as crystallization centers (Figure 4, *c*). The rate of crystallization of molten eutectic is higher than that in the alloy at argon-arc melting. This is indicated by finer grains, which do not separate in the remelted eutectic in zone 2 as they do in initial zone 3 in Figure 4. They create a rough surface, scatter the light and are seen as a continuous dark phase.

Obtained facts show that, on the one hand, despite the melting features, 36Nb–16Cr–16Ti–16Zr–16Al alloy is close to the eutectic ones. On the other hand, however, dendrites can precipitate in it at crystallization. Here, the ratio of the quantity of dendrites and eutectic can change, depending on the cooling rate.

Such a combination of properties can be explained as follows. In multicomponent alloys with a high mixing antropy the diffusion processes are slowed down. It, obviously, complicates achievement of the equilibrium during crystallization. Dendrites precipitate in the form of nonequilibrium, niobium-enriched bcc solid solution. Change of the melt chemical composition, accordingly, leads to a change of the chemical composition of the phases, which form a eutectic of a new composition. The data of X-ray phase analysis lead to the conclusion that the eutectic is formed by bcc solid solution, depleted in niobium, and solid solution based on Laves $ZrCr_2$ phase. Change in the chemical composition of these components can change the composition and properties of the precip-

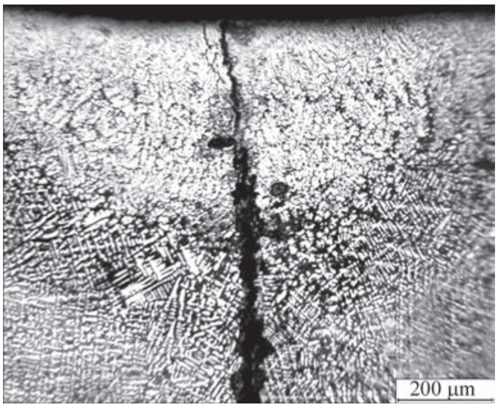

Figure 5. Defects in the form of cracks and pores in the welded joint of multicomponent high-entropy 36Nb–16Cr–16Ti–16Zr–16Al alloy 1.8 mm thick produced by laser welding at laser power of 400 W and welding speed of 0.833 mm/s (50 mm/min)

itating eutectic. Thus, kinetics of the diffusion processes can lead both to precipitation of dendrites in the alloy of primary eutectic composition, and to a change in the ratio of the quantity of dendrites and eutectic at its nonequilibrium crystallization under the real conditions.

Mechanical testing for uniaxial static tension of butt joints of samples from 36Nb–16Cr–16Ti–16Zr–16Al alloy showed that the fracture site changes with respect to the weld location at the change of the parameters of the technological modes of laser welding. It turned out to be impossible to predict the fracture site, proceeding just from the features of structure formation in the weld area. Crack initiation was not unambiguously associated with any established structural zone (zones 1, 2, 3 in Figures 3 and 4). Material softening, which leads to fracture is influenced by the feature of distribution of residual thermal stresses that is determined by the mode of heat input and removal during welding. In practice, it is necessary either to practically establish the influence of laser radiation power, welding speed and conditions of heat removal on welding of the specific parts, or perform modeling of the temperature field and arising temperature stresses.

Proceeding from the results of analysis of the obtained data it was established that depending on the values of mode parameters, the possible characteristic defects of laser welding for multicomponent high-entropy 36Nb–16Cr–16Ti–16Zr–16Al alloy are as follows: cracks (Figure 5) and microcracks in the cast zone of the weld and in the HAZ; segregation of refractory elements along the crystallite boundaries; shrinkage cavities and cavities in the crater; pores, pore chains; lacks-of-fusion; lacks-of-penetration; undercuts; and excess convexity.

Formation of the majority of the above-listed defects is associated with the feature of non-equilibrium crystallization of multicomponent high-entropy high-temperature alloys. To prevent their formation, rational are the measures on optimization of the technological parameters, aimed at increasing the melt cooling rate, in order to produce a more equilibrium structure.

In the case of impossibility of solving the problem of defect formation by optimizing the parameters of laser welding process, it is necessary to take the following measures to eliminate these defects:

- to eliminate defects in the form of pores, pore chains, lacks-of-fusion, weld depression, lacks-of-penetration – rewelding of the weld, with addition of filler material (if required);
- to prevent formation of shrinkage cavities and crater cavities — use of run-off tabs, as well as program control of smooth increase of laser radiation power at the welding start and smooth decrease at the end;
- to eliminate undercuts and excess weld convexity — performance of additional remelting by a defocused beam.

Conclusions

Composition of multicomponent high-entropy 36Nb–16Cr–16Ti–16Zr–16Al alloy is close to eutectic ones. A feature of eutectic multicomponent alloys is their proneness to nonequilibrium crystallization with formation of dendrites, enriched in refractory components. The ratio of the quantity of dendrites and eutectic can change, depending on the cooling rate. By the data of X-ray phase analysis the eutectic is formed by bcc solid solution, depleted in niobium and solid solution, based on Laves $ZrCr_2$ phase. Nonequilibrium precipitation of dendrites is, obviously, facilitated by diffusion deceleration in high-entropy alloys. With increase of the cooling rate, the melt of 36Nb–16Cr–16Ti–16Zr–16Al alloy is prone to hardening with formation of a single-phase structure.

Formation of most of the defects in butt joints of 36Nb–16Cr–16Ti–16Zr–16Al alloy, produced by laser welding, is associated with the feature of nonequilibrium crystallization of multicomponent high-entropy high-temperature alloys. In order to prevent their formation, it is rational to take measures on optimization of technological parameters, aimed at increase of the melt cooling rate, in order to produce a more equilibrium structure.

1. Boyer, R.R., Cotton, J.D., Mohaghegh, M., Schafrik, R.E. (2015) Materials considerations for aerospace applications. *MRS Bulletin*, 40(**12**), 1055–1066. DOI: https://doi.org/10.1557/mrs.2015.278
2. Sanin, V.N., Ikornikov, D.M., Andreev, D.E. et al. (2017) Synthesis of cast high entropy alloys with a low specific gravity by centrifugal metallothermic SHS-methods. A*dvanced Materials and Technologies*, **3**, 24–33. DOI: https://doi.org/10.17277/amt.2017.03.pp.024-033

3. Küpper, D., Heising, W., Corman, G. et al. (2017) *Get ready for industrialized additive manufacturing.* DigitalBCG, Boston Consulting Group. https://www.bcg.com/publications/2017/lean-manufacturing-industry-4.0-get-ready-for-industrialized-additive-manufacturing
4. George, E.P., Raabe, D., Ritchie, R.O. (2019) High-entropy alloys. *Nature Reviews Materials*, 4(**8**), 515–534. DOI: https://doi.org/10.1038/s41578-019-0121-4
5. Senkov, O.N., Miracle, D.B., Chaput, K.J., Couzinie, J.P. (2018) Development and exploration of refractory high entropy alloys — A review. *J. of Materials Research*, 33(**19**), 3092–3128. DOI: https://doi.org/10.1557/jmr.2018.153
6. Zhang, W., Liaw, P. K., Zhang, Y. (2018) Science and technology in high-entropy alloys. *Sci. China Materials*, 61(**1**), 2–22. DOI: https://doi.org/10.1007/s40843-017-9195-8
7. Chang, X., Zeng, M., Liu, K., Fu, L. (2020) Phase engineering of high-entropy alloys. *Advanced Materials*, 32, (**14**), 1907226. DOI: https://doi.org/10.1002/adma.201907226
8. Yan, X., Zhang, Y. (2020) Functional properties and promising applications of high entropy alloys. *Scripta Materialia*, 187, 188–193. DOI: https://doi.org/10.1016/j.scriptamat.2020.06.017
9. George, E.P., Curtin, W.A., Tasan, C.C. (2020) High entropy alloys: A focused review of mechanical properties and deformation mechanisms. *Acta Materialia*, **188**, 435–474. DOI: https://doi.org/10.1016/j.actamat.2019.12.015
10. Senkov, O.N., Wilks, G.B., Scott, J.M., Miracle, D.B. (2011) Mechanical properties of Nb25Mo25Ta25W25 and V20Nb20Mo20Ta20W20 refractory high entropy alloys. *Intermetallics*, 19(**5**), 698–706. DOI: https://doi.org/10.1016/j.intermet.2011.01.004
11. Brodnikovsky, N.P., Kulakov, A.S., Krapivka, N.A. et al. (2016) *Electron Microscopy and Strength of Materials*, **22**, 20–30. http://www.materials.kiev.ua/publications/EMMM/2016/4.pdf
12. Zhao, Y.Y., Lei, Z.F., Lu, Z.P. et al. (2019) A simplified model connecting lattice distortion with friction stress of Nb based equiatomic high-entropy alloys. *Materials Research Letters*, 7(**8**), 340–346. DOI: https://doi.org/10.1080/21663831.2019.1610105
13. *Panina E.*, Yurchenko N., Zherebtsov S. et al. (2019) Laser beam welding of a low density refractory high entropy alloy. *Metals*, 9(**12**), 1351. DOI: https://doi.org/10.3390/met9121351
14. Lopes, J.G., Oliveira, J.P. (2020) A short review on welding and joining of high entropy alloys. *Metals*, 10(**2**), 212. DOI: https://doi.org/10.3390/met10020212
15. Kang, B., Lee, J., Ryu, H.J., Hong, S.H. (2018) Ultrahigh strength WNbMoTaV high-entropy alloys with fine grain structure fabricated by powder metallurgical process. *Materials Sci. and Eng.: A*, 712, 616–624. DOI: https://doi.org/10.1016/j.msea.2017.12.021

Received 21.04.2021